



## **Structural, Morphological and Optical Properties of Zinc Oxide Nanoparticles by Polymer Capping**

T. Anantha kumar<sup>1,3\*</sup>, S. Malathi<sup>2</sup>, C.V. Mythili<sup>2</sup>, M. Jeyachandran<sup>3</sup>

<sup>1</sup>Department of Chemistry, Merit Arts and Science College, Idaikal,  
Ambasamudram – 627602, TN, India

<sup>2</sup>Department of Chemistry, Rani Anna Govt. College for Women,  
Tirunelveli - 627008, TN, India

<sup>3</sup>PG & Research, Department of Chemistry, Sri Paramakalyani College,  
Alwarkurichi – 627412, TN, India.

**Abstract** : Structural, morphological and optical properties of zinc oxide nanoparticles by polymer capping were investigated. Polyvinyl alcohol (PVA) is used as capping agent. A zinc oxide nanoparticle was synthesized by precipitation method. The resulting nanoparticles were characterized by X-ray diffraction (XRD), Scanning Electron Microscopy (SEM), Energy Dispersive X-ray Analysis (EDAX), Atomic Force Microscopy (AFM), Transmission Electron Microscopy (TEM), UV-vis absorption spectroscopy and Fourier Transform Infrared Spectroscopy (FTIR). The optical properties of polymer capped zinc oxide nanoparticles were characterized by UV-visible spectroscopy. The XRD results revealed that the zinc oxide nanoparticles are highly crystalline, having the hexagonal wurtzite crystal structure. The SEM image showed that the nanoparticles prepared in this study were spherical in shape. The UV absorption edges exhibited a blue shift, which might be caused by nanosize effect. The nanocomposites size can be calculated from Debye-Scherrer's formula.

**Keywords** : ZnO nanoparticles, XRD, SEM, TEM, Optical, Polymer, UV-Visible spectroscopy.

### **1. Introduction**

In recent years, nanoscience and technology have potential applications in the field of science and technology. Particularly nanocrystalline materials are treated as the suitable material for those applications. Intensive investigations were carried out for most of the applications of these new classes of materials. Among the various nanocrystalline materials, ZnO with particle size in the range of several nm are treated as exclusively suitable material for various applications because of their unique properties<sup>1</sup>. The application of nanoparticles within size range of 1-100 nm has received significant attention due to their novel properties. Among several of nanoparticles, ZnO nanoparticles (ZnO NPs) have received more attention. ZnO is a wide band gap (3.37 eV), semiconductor having large excitation binding energy of 60 meV at room temperature

T. Anantha kumar *et al* /International Journal of ChemTech Research, 2018,11(08): 48-57.

DOI= <http://dx.doi.org/10.20902/IJCTR.2018.110805>

which is significantly larger than other materials and it has high transmittance and good electrical conductivity<sup>2-5</sup>. ZnO has attracted much interest as one of the multifunctional inorganic nanoparticles due to its unique combination of superior physical, chemical, biological, electrical, optical, long-term environmental stability, biocompatibility, low cost and non-toxic properties. Therefore, nano-ZnO can potentially be applied to gas sensors, photocatalyst for degradation of waste water pollutants, catalysts, semiconductors, varistors, piezoelectric devices, field-emission displays, ultraviolet (UV) photodiodes, surface acoustic wave (SAW) devices, UV-shielding materials, rubber, medical and dental materials, pigments and coatings, ceramic, concrete, antibacterial and bactericide, and composites<sup>6-12</sup>.

ZnO has been one of the most promising materials for electrical devices, including transparent conductive films, light emitting diodes and photocatalyst<sup>13-18</sup>. Moreover, because it has been chemically and optically stable and has a low toxicity, its use as a fluorescent label for bioimaging has been anticipated. When using nanoparticles for biomedical purposes, the prevention of the aggregation of nanoparticles and the nonselective adsorption of the protein has been a serious concern. Capping nanoparticles has been one of the most important methods used to solve these problems. The fluorescence of ZnO has been observed in the UV region due to the exciton luminescence of the band gap and in the visible region due to oxygen defects and/or interstitial zinc caused by UV excitation<sup>13,19-24</sup>. Studies of the capping of ZnO nanoparticles by polyvinyl pyrrolidone (PVP) or polyvinyl butyral (PVB) have been previously performed<sup>25-26</sup>. We have synthesized the ZnO nanoparticles by capping with polyvinyl alcohol (PVA).

In particular, the type of polymer and the timing of the addition of the polymer were examined as critical parameters. The advantages of capping nanoparticles by polymer molecules were the following: (1) the passivation of surface defects, which decreased the nonradiative recombination center, such as dangling bonds, and increased fluorescence intensity<sup>27-29</sup>; (2) the aggregation inhibition of nanoparticles by a steric effect; (3) the utilization of nanoparticles for a drug delivery system (DDS) by the improvement in immunoaffinity; and (4) the probability of surface functionalization of nanoparticle, such as targeting.

## 2. Experimental:

### 2.1. Synthesis of polymer capped zinc oxide (ZnO) nanoparticles:

The capping agent PVA is dissolved in 100 ml of distilled water and stirred at 90°C for one hour and then cooled to room temperature. 2.8754 g of ZnSO<sub>4</sub>·7H<sub>2</sub>O (0.1M) was dissolved in 100 mL of distilled water. Meanwhile, PVA solution was prepared and was added to ZnSO<sub>4</sub>·7H<sub>2</sub>O (0.1M) solution. Then 1.6802 g of NaHCO<sub>3</sub> (0.2 M) was prepared separately and was added drop wise into the above solution under constant stirring. After being stirred at room temperature for 2-3 hours, the as formed precipitates were filtered, washed with distilled water and ethanol and finally dried in hot air oven at 80°C to get PVA capped zinc oxide nanoparticles<sup>30</sup>.

### 2.2. Characterization of the synthesized semiconductor nanoparticles:

Nanoparticles are generally characterized by their size, morphology and surface charge, using such advanced microscopic techniques as X-ray Diffraction (XRD), scanning electron microscopy (SEM) with EDAX, transmission electron microscopy (TEM) and atomic force microscopy (AFM). The average particle diameter, their size distribution and charge affect the physical stability and the in vivo distribution of the nanoparticles.

#### 2.2.1. FTIR Spectroscopy:

Fourier transform infrared spectroscopy is a powerful tool for identifying types of chemical bonds in a molecule as an infrared absorption spectrum serves as a molecular fingerprint of the particular substance.

Fourier transform infrared spectroscopy first developed by astronomers in the early 1950s to study the infrared spectra of distant stars has now been developed into a very powerful technique for the detection of very weak signals from the environment noise. It is a simple mathematical technique to resolve a complex wave into its frequency components. The conventional IR spectrometers are not of much use for the far IR region (20 – 400 cm<sup>-1</sup>) as the sources are weak and the detectors insensitive. FTIR has made this energy limited region more

accessible. It has made the middle infrared ( $400\text{-}4000\text{ cm}^{-1}$ ) more useful. An infrared radiation spans a section of the electromagnetic spectrum having wave numbers roughly from  $3000\text{ to }10\text{ cm}^{-1}$  or wavelength from  $0.78\text{ to }1000\text{ }\mu\text{m}$ . Molecular bonds vibrate at various frequencies depending on the elements and type of bonds. For any given bond, there are several specific frequencies at which it can vibrate. The absorption is generally presented in the form of spectrum with wavelength or wave number as the X axis and absorption intensity or percent transmittance as the Y axis.

Identification of molecular constituents is done by assigning the experimentally observed bands to possible functional groups and stretching and bending vibrations of bonds. The technique works on the fact that bonds and groups of bonds vibrate at characteristic frequencies. A molecule that is exposed to infrared rays absorbs infrared energy at frequencies which are characteristic to that molecule. During FTIR analysis, a spot on the specimen is subjected to a modulated IR beam. The resulting FTIR spectral pattern is then analyzed and matched with known signature of identified materials.

### 2.2.2. UV –Vis Spectroscopy:

The synthesized semiconductor nanoparticles was monitored by using double beam UV-Vis spectrophotometer (Lambda 25, Perkin Elmer, Singapore) of the semiconductor wavelength range of  $200\text{ – }800\text{ nm}$  with  $1000\text{ mm}$  quartz cell. This resolution of the UV-Vis spectrophotometer was  $1\text{ nm}$ . The UV-Vis spectra of resulting solution were recorded. The spectrum is plotted for wavelength on X-axis against absorbance on Y-axis.

### 2.2.3. X-ray diffraction (XRD) analysis:

The particle size and nature of compound semiconductor and ternary semiconductor were determined using XRD. This was carried out using Shimadzu XRD-6000/6100 model with  $30\text{ kv}$ ,  $30\text{ mA}$  with  $\text{Cu } k\alpha$  radians at  $2\theta$  angle. With the X-ray powder diffraction, a rapid analytical technique, primarily used for phase identification of a crystalline material and provide information on unit cell dimensions. The analyzed material is finely ground and average bulk composition is determined. The size of the particle on the compound and ternary semiconductor were determined by using Debye Scherrer's equation.

$$D = \frac{0.94\lambda}{\beta \cos\theta} \text{-----(1)}$$

Where

D is the mean size of the ordered (crystalline) domains, which may be smaller or equal to the grain size.

$\lambda$  is the wavelength

$\beta$  is the line broadening at half the maximum intensity (FWHM), after subtracting the instrumental line broadening in radians.

### 2.2.4. Scanning Electron microscopy (SEM):

Scanning electron microscopy (SEM) is giving morphological examination with direct visualization. The techniques based on electron microscopy offer several advantages in morphological and sizing analysis; however, they provide limited information about the size distribution and true population average. For SEM characterization, nanoparticles solution should be first converted into a dry powder, which is then mounted on a sample holder followed by coating with a conductive metal, such as gold, using a sputter coater. The sample is then scanned with a focused fine beam of electrons<sup>31</sup>. The surface characteristics of the sample are obtained from the secondary electrons emitted from the sample surface. The nanoparticles must be able to withstand vacuum, and the electron beam can damage the polymer. The mean size obtained by SEM is comparable with results obtained by dynamic light scattering. Moreover, these techniques are time consuming, costly and frequently need complementary information about sizing distribution<sup>32</sup>.

### 2.2.5. Transmission electron microscope (TEM):

TEM operates on different principle than SEM, yet it often brings same type of data. The sample preparation for TEM is complex and time consuming because of its requirement to be ultra thin for the electron transmittance. The nanoparticles dispersion is deposited onto support grids or films. To make nanoparticles withstand the instrument vacuum and facilitate handling, they are fixed using either a negative staining material, such as phosphotungstic acid or derivatives, uranyl acetate, etc, or by plastic embedding. An alternate method is to expose the sample to liquid nitrogen temperatures after embedding in vitreous ice. The surface characteristics of the sample are obtained when a beam of electrons is transmitted through an ultra thin sample, interacting with the sample as it passes through<sup>32</sup>.

### 2.2.6. Atomic force microscopy (AFM):

Atomic force microscopy (AFM) offers ultra-high resolution in particle size measurement and is based on a physical scanning of samples at sub-micron level using a probe tip of atomic scale<sup>33</sup>. Instrument provides a topographical map of sample based on forces between the tip and the sample surface. Samples are usually scanned in contact or noncontact mode depending on their properties. In contact mode, the topographical map is generated by tapping the probe on to the surface across the sample and probe hovers over the conducting surface in non-contact mode. The prime advantage of AFM is its ability to image non-conducting samples without any specific treatment, thus allowing imaging of delicate biological and polymeric nano and microstructures<sup>34</sup>. AFM provides the most accurate description of size and size distribution and requires no mathematical treatment. Moreover, particle size obtained by AFM technique provides real picture which helps understand the effect of various biological conditions<sup>35</sup>.

## 3. Results and Discussions:

### 3.1. XRD Analysis:

The structural analysis of the polymer capped zinc oxide nanoparticles was carried out using Cu-K $\alpha$  radiation having wavelength 1.5406 Å. The X-ray diffraction patterns of the synthesized zinc oxide nanoparticles by using poly vinyl alcohol (PVA) used as capping agent was further demonstrated and confirmed by the characteristic peaks observed with XRD image (Fig.1) phase identification is accomplished by comparing the data (peaks and relative intensities) from the specimen with peaks and relative intensities from a very large set of standard data provided by the International Center for Diffraction Data (ICDD).

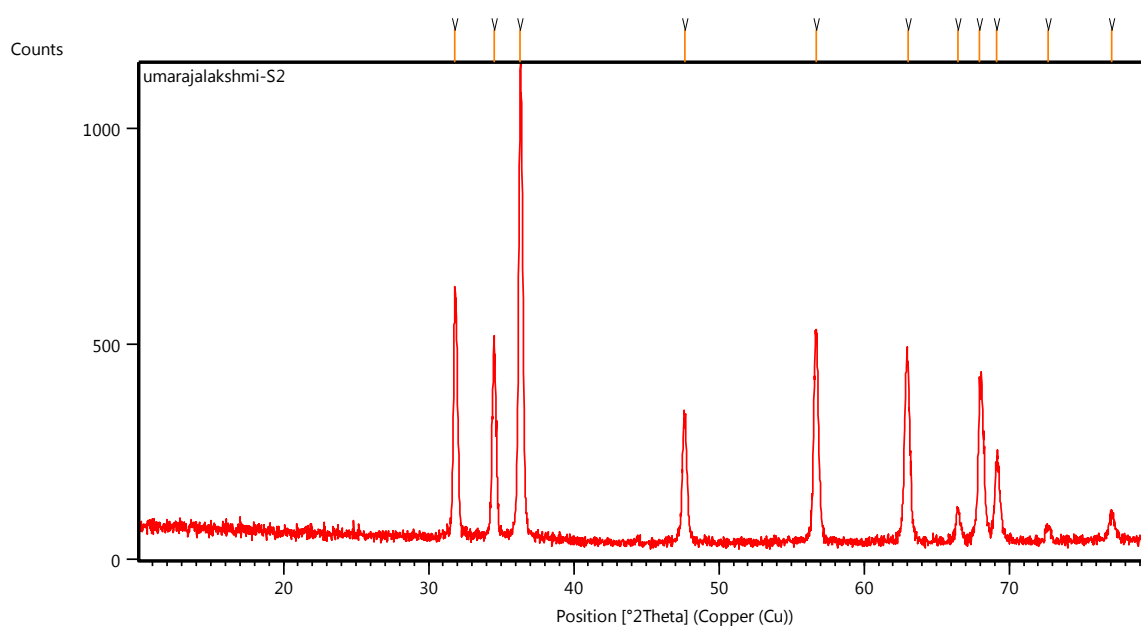


**Fig. 1. XRD spectrum of PVA capped Zinc oxide nanoparticles**

All of the indexed peaks in the obtained spectrum are well matched with that of bulk zinc oxide (JCPDS code no. 36-1451), which confirms that the synthesized nanoparticles have wurtzite hexagonal structure with high purity. The different peak orientations were observed along the (100), (002), (101), (102) and (110) planes. The typical hexagonal wurtzite structure of the synthesized zinc oxide nanoparticle is inferred from the XRD pattern, which is in good agreement with the intrinsic fundamental structure of zinc oxide as reported in the literature. This result suggests that the growth of PVA capped ZnO is good. The information on the particle size (A) of PVA capped ZnO nanoparticles have been obtained from the following Scherrer relations.

$$D = \frac{0.94\lambda}{\beta \cos\theta} \quad (1)$$

Where D is the average crystallite size,  $\lambda$  is the wavelength of incident X-ray ( $1.5418 \text{ \AA}$ ),  $\beta$  is the full width half maximum (FWHM) of X-ray diffraction expressed in radian and  $\theta$  is the position of the diffraction peak in the diffractograms. The particle size was found to be 41.5 nm.

### 3.2. SEM with EDAX Analysis:

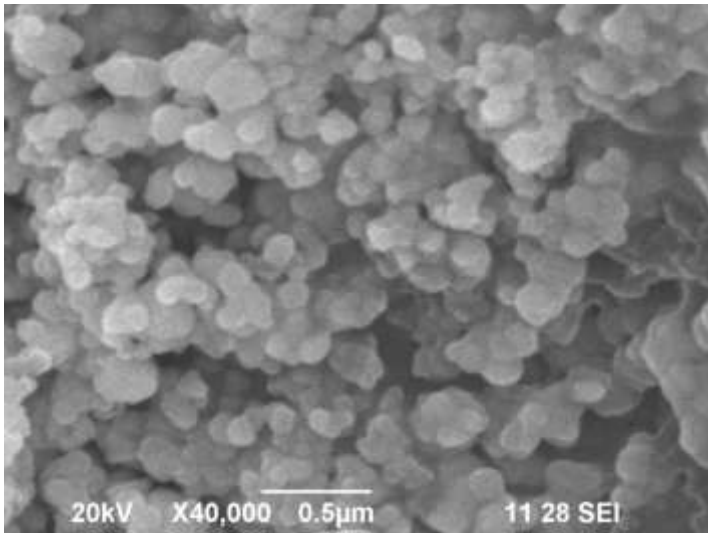


Fig. 2. SEM image of PVA capped Zinc oxide nanoparticles

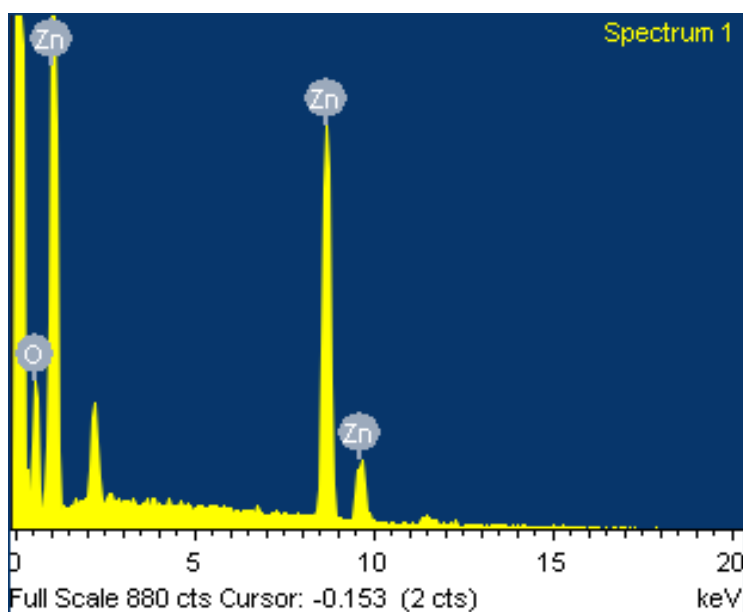


Fig. 3. EDAX spectra of PVA capped Zinc oxide nanoparticles

The surface morphology of the synthesized PVA capped zinc oxide nanoparticles was identified on nanoscale by Scanning Electron Microscope. SEM image had shown shape and distribution of the zinc oxide nanoparticles synthesized by polymer capping. The polymer capped zinc oxide nanoparticles were obtained as nanospheres with the particle size of 40 -50 nm which proves the role of polymer capping in the size and morphology of zinc oxide nanoparticles (Fig. 2). The PVA was used as a capping agent, which prevents the nanoparticles to aggregate. It is proved that the prevention of aggregation of nanoparticles in the presence of the surfactant is more effective. This capping agent's molecules bind to the surface of the particle by stabilizing the nuclei and larger nanoparticles against aggregation, hence controlling the growth of nanoparticles. This fact confirms the results of XRD analysis. The present report is well matched with sudha *et al*<sup>30</sup>. The EDAX spectra of PVA capped zinc oxide nanoparticles are presented in Fig.3. The peaks corresponding to Zn and O are clearly observed in the EDX spectrum at their normal energy and the results are clearly indicating the formation of zinc oxide nanoparticles.

### 3.3. AFM Analysis:

Atomic force microscopy (AFM) is also known as scanning force microscopy (SFM). AFM is a basic technique and inevitable for all nanoscopic research. The AFM image of PVA capped zinc oxide nanoparticles is shown in figure.8. Surface topological features of polymer capped ZnO samples as-observed under AFM 3D is shown in figures 4. The micrograph at  $3.45 \mu\text{m} \times 3.45 \mu\text{m}$  exhibit an uniform surface with cone like grains covering the ZnO surface can be seen for this sample. The surface roughness, RMS average value and heights were determined by AFM analysis. The surface roughness was found to be in the range of  $1.56 \mu\text{m}$  to  $2.12 \mu\text{m}$ . The surface roughness of the samples was increased in the presence of polymer capping agent due to the presence of functional groups.

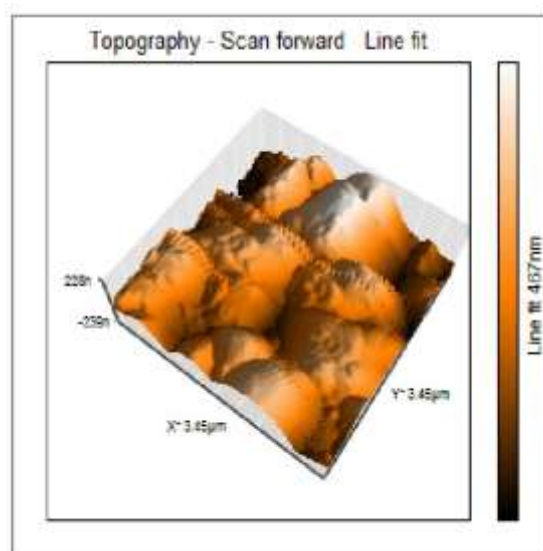
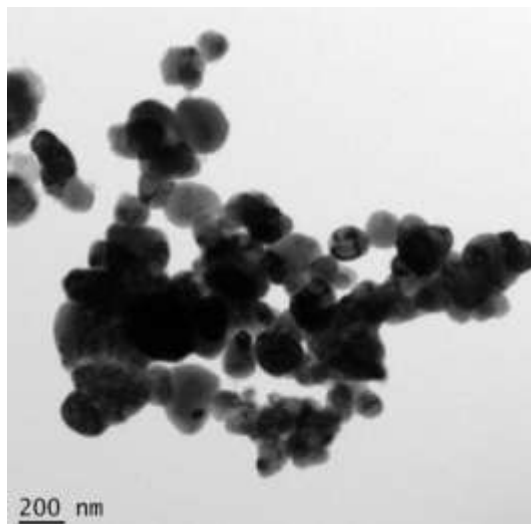


Fig. 4. AFM 3D image of PVA capped Zinc oxide nanoparticles

### 3.4. TEM analysis:

The obtained polymer capped zinc oxide nanoparticles are further characterized by transmission electron microscope. The shape and size of the sample is investigated using TEM analysis. Figure.5. shows the TEM image of PVA capped zinc oxide nanoparticles, in which physical separation of the particles was maintained during processing, thus preventing the formation of agglomerates. Besides, one can also observe that around the zinc oxide nanospheres there encircle some shadows, implying the existence of capped PVA. This is due to the fact that PVA can form a shell surrounding the particles to prevent them from being large in size by means of aggregation. The particle size is around 40-50 nm.



**Fig. 5. TEM image of PVA capped Zinc oxide nanoparticles**

### 3.5. Optical Analysis:

The optical property of the sample was characterized by UV–Vis spectroscopy. The optical absorption spectrum of the polymer ZnO sample was recorded at room temperature in the wavelength range between 200 and 800 nm and is shown in Fig. 6. The absorption data were analyzed using the classical relation for near edge optical absorption of semiconductors.

$$\alpha = \frac{A(h\nu - E_g)^n}{h\nu}$$

Where  $h\nu$  is the photon energy.  $A$  and  $n$  are constants. Where  $n$  is 2 for a direct energy gap and  $\frac{1}{2}$  for an indirect energy gap. The plot of  $(\alpha h\nu)^2$  vs.  $h\nu$  is shown in **Fig.11**. Extrapolating the straight line of this plot for zero absorption coefficients it gives the direct band gap of nanostructure materials.

The absorption band gap edge was shifted to shorter wavelength and the corresponding band gap is 3.6 eV for PVA capped ZnO nanomaterial. It is well known that the absorption edge is related to the size of the nanoparticles. The absorption edge of the ZnO nanoparticles shows a blue-shift as compared with the value for bulk ZnO nanoparticles. This blue shift could be attributed to the size reduction effect of PVA capped zinc oxide nanoparticles and structural defect of nanomaterials. The capping agent is used to arrest the growth of nanoparticles and to stabilize them from aggregation. The capping agent also modifies the structural, morphological and optical properties of nanoparticles<sup>36</sup>. Many investigations have reported the optical gap of zinc oxide nanoparticles.

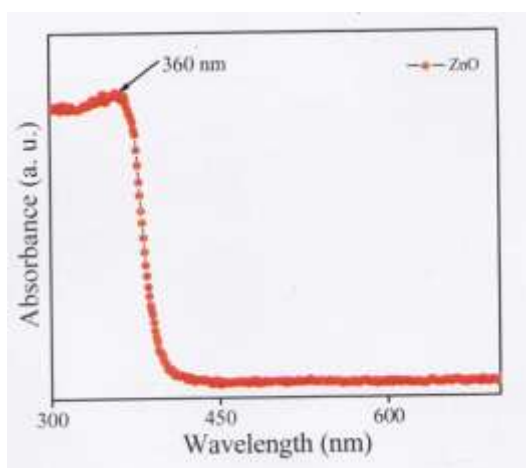


**Fig. 6. UV-Vis spectrum of PVA capped Zinc oxide nanoparticles**

### 3.6. FTIR Analysis:

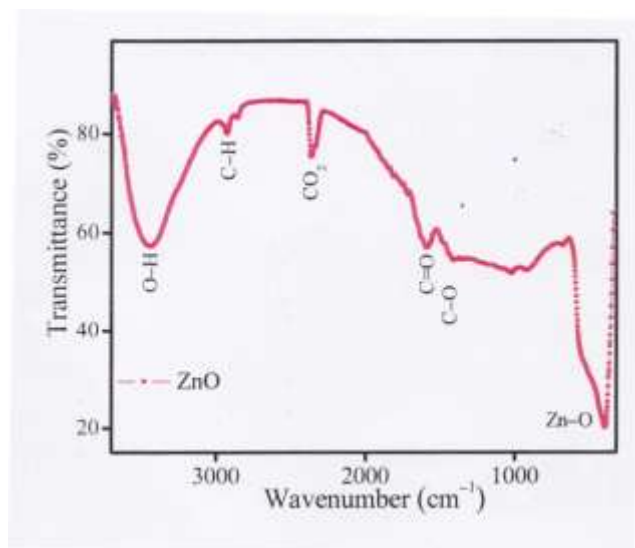


**Fig. 7. FTIR Spectrum of PVA capped Zinc oxide nanoparticles**

FTIR spectrum of the synthesized polymer capped zinc oxide nanoparticle is given in the Fig.7. The vibrational mode at  $391\text{ cm}^{-1}$  corresponds to Zn-O absorption in the hexagonal type ZnO. Two principle peaks are observed at  $1425\text{ cm}^{-1}$  and  $1586\text{ cm}^{-1}$  corresponding to the symmetric stretching of C-O bond and strong asymmetric stretching of C=O bond, respectively<sup>37</sup>. The bond observed at  $2361\text{ cm}^{-1}$  is due to  $\text{CO}_2$  molecule in air<sup>38</sup>. Vibrational mode observed at  $2925\text{ cm}^{-1}$  is due to C-H stretching vibration. The characteristic band at  $3437\text{ cm}^{-1}$  corresponds to the stretching vibration of O-H groups. It should be noted that, these O-H groups are present in the sample even after drying. This indicates that the O-H complexes are associated with different defects and increased free-carrier concentration.

#### 4. Conclusion:

The synthesis of zinc oxide (ZnO) nanoparticle using PVA as capping agent was carried out by precipitation method at room temperature. Structural characterization was done by XRD. The XRD result revealed the hexagonal wurtzite structure of ZnO. The particle size was found to be 41.5 nm. The calculated lattice parameters agreed well with the JCPDS data. In SEM and EDAX analysis, the polymer capped zinc oxide nanoparticles were obtained as nanospheres with the particle size of 40-50 nm which proves the role of polymer capping in the size and morphology of zinc oxide nanoparticles and the peaks corresponding to Zn and O are clearly observed in the EDX spectrum at their normal energy and the results are clearly indicating the formation of zinc oxide nanoparticles. The micrograph at exhibit an uniform surface with cone like grains covering the ZnO surface can be seen for this sample. The surface roughness, RMS average value and heights were determined by AFM analysis. TEM image of PVA capped zinc oxide nanoparticles, in which physical separation of the particles was maintained during processing, thus preventing the formation of agglomerates. Besides, one can also observe that around the zinc oxide nanospheres there encircle some shadows, implying the existence of capped PVA. The particle size is around 40-50 nm. The optical properties of polymer capped zinc oxide were studied by UV-Vis analysis. The UV-Vis absorption spectrum shows strong UV absorption and high transparency in the visible region. The spectrum showed blue shift when compared with bulk zinc oxide, which confirms the quantum confinement in zinc oxide nanoparticles. The vibrational modes of zinc oxide nanoparticles were studied from FTIR analysis. The synthesized zinc oxide nanoparticle is a promising candidate for the applications in various fields especially in water purification.

#### References:

1. Wang L, Muhammed M. Synthesis of zinc oxide nanoparticles with controlled morphology. *J. Mater Chem.*,1999, 9; 2871-2878.
2. Srivastava V, Gusain D, Sharma YC. Synthesis, characterization and application of zinc oxide nanoparticles (n-ZnO). *Ceram Int.*, 2013, 39; 9803-9808.



3. Cao GZ. Growth of zinc oxide nanorod arrays through sol electrophoretic deposition. *The J. Phy. Chem.*, 2004, 108; 19921-19931.
4. Zhou WD, Wu X, Zhang YC. Solvothermal synthesis of hexagonal ZnO nanorods and their photoluminescence properties. *Mater Lett.*, 2007, 61; 2054-2057.
5. Hu SH, Chen YC, Hwang CC, Peng CH, Gong DC. Development of a wet chemical method for the synthesis of arrayed ZnO nanorods. *J. Alloys and Compd.*, 2010, 500; 117-121.
6. Xiong M, Gu G, You B, Wu L. Preparation and Characterization of poly(styrene butylacrylate) latex/nano-ZnO nanocomposites. *J. Appl Polym Sci.*, 2003, 90; 1923-1931.
7. El-Kemary M, El-Shamy H, El-Mehasseb I. Photocatalytic degradation of ciprofloxacin drug in water using ZnO nanoparticles. *J. Lumi.*, 2010,130,2327-2331.
8. Moezzi A, McDonagh A-M, Cortie MB. Zinc oxide particles: synthesis, properties and applications. *Chem. Eng. J.*, 2012,185-186; 1-22.
9. Schmidt-Mendel L, MacManus-Driscoll JL. ZnO nanostructures; defects and devices. *Mater.Today.*, 2007, 10; 40-48.
10. Ma X-Y, Zhang W-D. Effects of flower-like ZnO nanowhiskers on the mechanical, thermal and antibacterial properties of waterborne polyurethane. *Polym. DegradStab.*, 2009, 94; 1103-1109.
11. Li YQ, Fu SY, Mai YW. Preparation and characterization of transparent ZnO/epoxy nanocomposites with high-Uv shielding efficiency. *Polym.*,2006, 47;2127-2132.
12. Li YO, Yang Y, Fu SY. Photo-stabilization properties of transparent inorganic UV-filter/epoxy nanocomposites. *Compos. Sci Technol.*, 2007, 67;3465-3471.
13. Vanheusden K, Seager CH, Warren WL, Tallant DR, Voigt JA. Correlation between photoluminescence and oxygen vacancies in ZnO phosphors. *Appl. Phys. Lett.*,1996, 68, 403-405.
14. Dayan NJ, Sainkar SR, Karekar RN, Aiyer RC. Formulation and characterization of ZnO: Sb thick-film gas sensors. *Thin Solid Films.*,1998, 325, 254-258.
15. Chen CS, Kuo CT, Wu TB, Lin IN. Microstructures and electrical properties of V2O5-based multicomponent ZnO varistors prepared by microwave sintering process. *Jpn. J. Appl. Phys. Part 1.*,1997, 36, 1169-1175.
16. Gorla CR, Emanetoglu NW, Liang S, Mayo WE, Lu Y, Wraback M, Shen H. Structural, optical, and surface acoustic wave properties of epitaxial ZnO films grown on (0112) sapphire by metalorganic chemical vapor deposition. *J. Appl. Phys.*,1999, 85, 2595-2602.
17. Tang ZK, Wong GKL, Yu P, Kawasaki M, Ohtomo A, Koinuma H, Segawa Y. Room-temperature ultraviolet laser emission from self-assembled ZnO microcrystallite thin films. *Appl. Phys. Lett.*,1998, 72, 3270-3272.
18. Reynolds DC, Look DC, Jogai B. Optically pumped ultraviolet lasing from ZnO. *Solid State Commun.*,1996, 99, 873-875.
19. Liu M, Kitai AH, Mascher P. Point-defects and luminescence-centers in zinc-oxide and zinc-oxide doped with manganese. *J. Lumin.*,1992, 54, 35-42.
20. Vanheusden K, Warren WL, Seager CH, Tallant DR, Voigt JA, Gnade BE. Mechanisms behind green photoluminescence in ZnO phosphor powders. *J. Appl. Phys.*,1996, 79, 7983-7990.
21. Li D, Leung YH, Djuricic AB, Liu ZT, Xie MH, Shi SL, Xu SJ, Chan WK. Different origins of visible luminescence in ZnO nanostructures fabricated by the chemical and evaporation methods. *Appl. Phys. Lett.*,2004, 85, 1601-1603.
22. Djuricic AB, Choy WCH, Roy VAL, Leung YH, Kwong CY, Cheah KW, Rao TKG, Chan WK, Lui HT, Surya C. Photoluminescence and electron paramagnetic resonance of ZnO tetrapod structure. *Adv. Funct. Mater.*,2004, 14, 856-864.
23. Garces NY, Giles NC, Halliburton LE, Cantwell G, Eason DB, Reynolds DC, Look DC. Production of nitrogen acceptors in ZnO by thermal annealing. *Appl. Phys. Lett.*,2002, 80, 1334-1336.
24. Xu PS, Sun YM, Shi CS, Xu FQ, Pan HB. The electronic structure and spectral properties of ZnO and its defects. *Nucl. Instrum. Methods Phys. Res.*,2003, 199, 286-290.
25. Guo L, Yang S.H, Yang C.L, Yu P, Wang JN, Ge WK, Wong GKL. Highly monodisperse polymer-capped ZnO nanoparticles: Preparation and optical properties. *Appl. Phys. Lett.*,2000, 76, 2901-2903.
26. Guo L, Yang S.H, Yang CL, Yu P, Wang JN, Ge WK, Wong GKL. Synthesis and characterization of poly(vinylpyrrolidone)-modified zinc oxide nanoparticles. *Chem. Mater.*,2000, 12, 2268-2274.
27. Pankove JI. *Optical Processes in Semiconductors*; Dover Publications: New York, NY, USA, 1971.
28. Micic OI, Sprague JR, Lu Z, Nozik A. Highly efficient band-edge emission from InP quantum dots. *Appl. Phys. Lett.*,1996, 68, 3150-3152.

29. Kuno, M, Lee, J.K, Dabbousi, B.O, Mikulec, F.V,Bawendi, M.G. The band edge luminescence of surface modified CdSenanocrystallites: Probing the luminescing state. J. Chem. Phys.,1997, 106, 9869-9882.
30. Sudha M, Senthilkumar S, Hariharan R, Suganthi A,Rajarajan M. Synthesis, Characterization and study of Photocatalytic activity of surface modified ZnO nanoparticles by PEG capping. J. Sol-Gel Sci. Technol., 2013, 65; 301-310.
31. Jores K, Mehnert W, Drecusler M, Bunyes H, Johan C, MAdler K. Investigation on the stricter of solid lipid nanopartuicles and oil-loaded solid nanoparticles by photon correlation spectroscopy, fieldflowfractionasition and transmission electron microscopy. J Control Release., 2004, 17; 217- 227.
32. Molpeceres J, Aberturas MR, Guzman M. Biodegradable nanoparticles as a delivery system for cyclosporine: preparation and characterization. J Microencapsul. 2000, 17; 599-614.
33. Muhlen AZ, Muhlen EZ, Niehus H, Mehnert W. Atomic force microscopy studies of solid lipid nanoparticles. Pharm Res.,1996, 13; 1411- 1416.
34. Shi HG, Farber L, Michaels JN, Dickey A, Thompson KC, Shelukar SD, Hurter PN, Reynolds SD, Kaufman MJ. Characterization of crystalline drug nanoparticles using atomic force microscopy and complementary techniques. Pharm Res.,2003, 20; 479 – 484.
35. Polakovic M, Gorner T, Gref R, Dellacherie E. Lidocaine loaded biodegradable nanospheres. II. Modelling of drug release. J Control Release., 1999, 60; 169 -177.
36. Abbas Rahdar. Study of different capping agent effect on the structural and optical properties of Mn doped ZnS nanostructures, World Appl. Program., 2013, 3; 56-60.
37. Xue ZY, Zhang DH, Wang QP, Wang JH. The blue photoluminescence emitted from ZnO films deposited on glass substrate by rf magnetron sputtering, Appl. Surf. Sci., 2002, 195; 126-129.
38. Fu ZX, Guo CX, Lin BX, Liao GH. Cathodoluminescence of ZnO films, Chinese Phys. Lett., 1998, 15; 457-459.

\*\*\*\*\*